Deep Reflection Prior

Qingnan Fan^{1*} Yingda Yin^{2*} Dongdong Chen³ Yujie Wang⁴ Angelica Aviles-Rivero⁵
Ruoteng Li⁶ Carola-Bibiane Schnlieb⁵ Dani Lischinski⁷ Baoquan Chen²

¹Stanford University ²Peking University ³Microsoft ⁴Shandong University

⁵Cambridge University ⁶National University of Singapore ⁷The Hebrew University of Jerusalem

Abstract

Reflections are very common phenomena in our daily photography, which distract people's attention from the scene behind the glass. The problem of removing reflection artifacts is important but challenging due to its ill-posed nature. Recent learning-based approaches have demonstrated a significant improvement in removing reflections. However, these methods are limited as they require a large number of synthetic reflection/clean image pairs for supervision, at the risk of overfitting in the synthetic image domain. In this paper, we propose a learning-based approach that captures the reflection statistical prior for single image reflection removal. Our algorithm is driven by optimizing the target with joint constraints enhanced between multiple input images during the training stage, but is able to eliminate reflections only from a single input for evaluation. Our framework allows to predict both background and reflection via a one-branch deep neural network, which is implemented by the controllable latent code that indicates either the background or reflection output. We demonstrate superior performance over the state-of-the-art methods on a large range of real-world images. We further provide insightful analysis behind the learned latent code, which may inspire more future work.

1. Introduction

Reflection is commonly observed when taking photos through a piece of glass due to the interference between reflected light and the light coming from the background scene. These reflection artifacts significantly degrade the visibility of target scene, and distract users from focusing on it. Therefore, removing reflections is a problem of great interest for many computer vision and graphics applications.

To deal with this problem, the most common solution, in terms of traditional vision-based approaches, is to leverage the relation from multiple input images, such as the motion video sequence [35] and flash/non-flash image pair [1]. Another set of techniques [16, 38] rely on strong priors applied on the background or reflection layer from a single input. Due to the use of hand-crafted features, the traditional methods tend to fail in some challenging cases where prior assumptions are violated. In addition, they suffer from slow running speed due to the iterative optimization process.

Inspired by the tremendous success of deep learning in many image processing tasks, a variety of recent works [6, 39, 30, 36, 32, 33] have focused on learning-based solutions for reflection removal by taking use of the synthetic reflections as training signals. These techniques have proven to boost the overall performance significantly and achieve state-of-the-art results. Despite their success, by directly supervising the synthetic labels, the network may learn limited transferable knowledge and generalizes weakly in the real test data as observed in many previous work [5, 24, 14, 26].

To alleviate such a difficulty, in this paper, we propose a deep learning approach for reflection removal that requires neither ground truth data for supervision, nor hand-crafted priors designed for the non-learning approaches. Instead, it learns a better deep learning prior for reflection images. Our framework builds on an implicit connection between multi-image and single-image methods. Our algorithm learns to benefit from the inner constraints between multiple input images during training, but is capable of removing the reflections from a single input during evaluation.

Our framework is implemented via a single-branch fully convolutional neural network (FCN) with only one input and one output, which is however able to predict the background and reflection layer simultaneously. To this aim, a latent code within the FCN is learned dynamically to control the background or reflection prediction. As reflection removal is under-constrained, we build on a joint combination of multiple label-free objective functions to limit the solution space and help the convergence of the deep network. Optimized with our deep learning framework, we demonstrate superior quantitative and qualitative performance over the state-of-the-art reflection removal approaches on vari-

^{*}Equal Contribution

ous real reflection cases.

Our contributions in this paper can be summarized as follows:

- We present a learning-based solution to reflection removal, which does not take advantage of the ground truth supervision signal, but is able to learn a better deep reflection prior for real image improvement. Our algorithm benefits from multiple inputs during training, but only requires a single input for evaluation.
- We develop a single-branch fully convolutional neural network, which is controlled by the learned latent code that determines the background or reflection prediction. In absence of ground truth data, we jointly train our network on a variety of objective functions to aid the learning process.
- Our proposed algorithm outperforms state-of-the-art supervised approaches on various kinds of challenging real-world reflection images.

2. Related Work

Reflection removal has been widely explored in the community. The body of literature can be roughly classified into two categories: the non-learning approaches and learning based approaches.

Non-learning approaches. Since reflection removal is a highly underdetermined problem, approaches leverage on different type of priors to deal with this problem. A set of approaches are oriented to use multiple input images [7, 25, 18, 8, 15, 22, 9, 35, 37, 17, 38]. These techniques require that the scene being captured from different viewpoints. They exploit the motion cue, which assumes the background and foreground motion is usually different due to visual parallax. The exhibit motion is usually represented by either parametric models [9, 8] or dense motion fields [35, 25]. Some other approaches take a sequence of images using special devices in different environments, such as those take multiple polarized images with angular filters to find the optimal separation [10, 20, 18], or the ones with repetitive dynamic behaviors and different illuminations. Some researchers exploit multiple images taken under special conditions and camera settings, such as using flash/non-flash image pair [1], focus/defocus image pair [19], etc. Due to the additional information obtained from multiple images, this problem becomes less ill-posed. However, the special data requirement limits these methods from more practical application scenarios.

Another set of techniques rely on the use of single input image [12, 13, 28, 2, 38]. These approaches leverage the gradient sparsity prior for layer decomposition, which is further assisted with interactive user annotation to improve the separation performance [11, 23]. As the reflection

and background layers are usually at different depth, the reflection plane is very likely to remain outside the depth of field (DOF) and hence becomes blurry. The approaches of [16, 31] incorporate priors explicitly into the objective function to be optimized. A more realistic physics model takes the thickness of glass into consideration, where ghosting effects are adopted into a specially designed image formation formula [21].

Learning approaches. The first deep learning solution was presented in [6]. It relied on the common assumption of blurry reflection to develop a novel reflection image synthesis method. Authors of that technique proposed a two-stage framework to predict the sparse image structure as the guidance for the background recovery. Similarly, [39] followed their data generation approach, and designed a context aggregation network with perceptual loss for reflection separation. Unlike [6] that combines edge and image learning sequentially, [30] proposed a novel reflection removal framework that unifies gradient inference and image reconstruction in a concurrent way. In that work, authors acquired a reflection image dataset (RID) to facilitate the training data synthesis. Authors in [36] developed a bidirectional neural network to enable the mutual benefit between background and reflection estimation.

All the aforementioned deep learning solutions are based on single input image. Recently, [34] proposed to learn from multiple polarized images, along with a novel synthetic data generation approach, which accurately simulates reflections in polarized images. [3] proposed to train their network with multiple input images and one ground truth label for supervised learning, and applied the trained network for single image reflection removal during evaluation.

Unlike the previous non-learning or learning approaches, our algorithm takes advantage of methods of both types, that is: we leverage multiple input images in the training stage to ease the ill-posedness, while learning a general parametric solution in the absence of ground truth as direct supervision signal, which requires less hand-crafted features and only a single input during evaluation.

3. Overall Framework

The overall framework is shown in Figure 1. In the training phase, our algorithm takes two reflection images as input (I_1,I_2) , which are forwarded into the same reflection removal network independently to predict their corresponding background and reflection layers $(\{\hat{B}_1,\hat{R}_1\},\{\hat{B}_2,\hat{R}_2\})$. The reflection layers (\hat{R}_1,\hat{R}_2) are composed with every other background layer (\hat{B}_1,\hat{B}_2) to generate a set of reflection images denoted as $(\hat{I}_{11},\hat{I}_{12},\hat{I}_{21},\hat{I}_{22})$.

Although this framework supports separation of background and reflection, without ground truth supervision or specific constraints on the output, this in itself cannot determine the appearance of background and reflection layer as

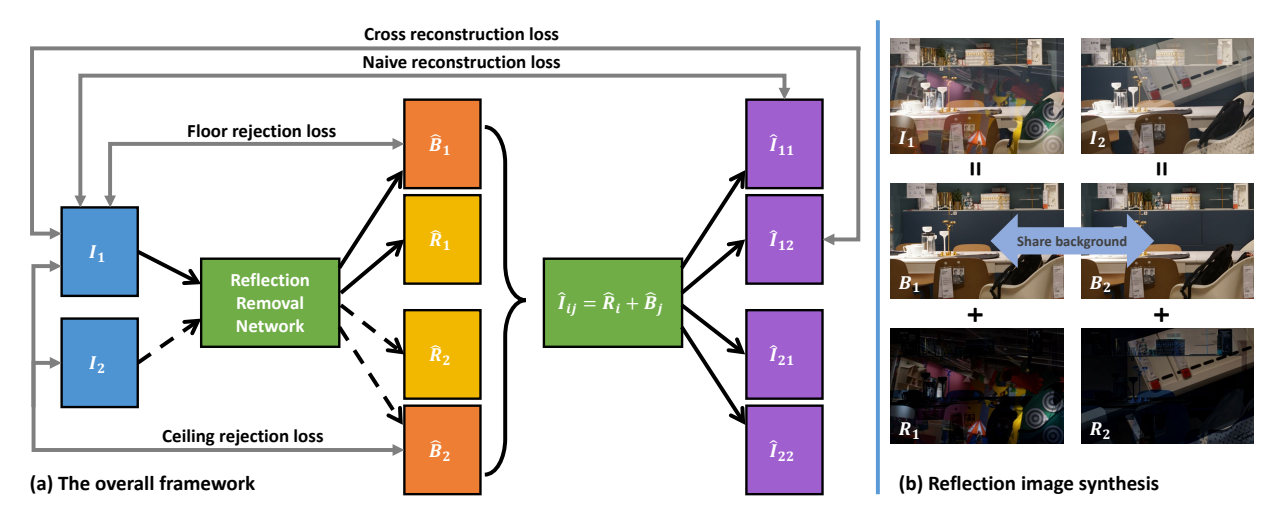


Figure 1. Our overall framework for reflection removal. (a) Illustration of the proposed algorithm. The deep network is fed with a pair of reflection images, and decompose them into corresponding background and reflection layers, which are further composed into new reflection images. We append a joint objective of four loss functions on all the predictions for optimization in absence of ground truth. Since the input images are forwarded into the deep network individually, during evaluation, our framework is able to take a single input to generate the clean image. Note the framework is symmetric and for clarity we omit similar lines. (b) The corresponding reflection image synthesis pipeline. The two inputs are composed of the same background image.

there are arguably countless feasible solutions to the reflection image formation model as shown below.

Reflection Image Synthesis. Given a background (B) and a reflection (R) layer¹, the corresponding reflection image (I) is a linear combination as I=B+R. Therefore to prepare for multi-image reflection removal, we build an inner connection between the different input reflection images, which reads:

$$I_i = B_i + R_i \tag{1}$$

$$B_1 = B_2 = \dots = B_n \tag{2}$$

where i indicates one specific reflection image among all the n inputs. It means that all the input reflection images share the same background, and differentiate only in the reflection layer. In order to force the network to perform the desired separations, we incorporate an objective combined with four loss functions that take use of the special data configuration to jointly train our deep network.

Naive Reconstruction Loss. Given the decomposed background and reflection layer, the most straightforward supervision can be applied by minimizing the per-pixel difference between the recomposed reflection image and the original input samples as,

$$\mathcal{L}_{naive} = ||\hat{I}_{11} - I_1||_2^2 + ||\hat{I}_{22} - I_2||_2^2$$
 (3)

where \hat{I}_{ij} is synthesized via $\hat{I}_{ij} = \hat{R}_i + \hat{B}_j$. Despite this objective already reduces the solution space greatly, it is still unclear which one of the two outputs should be background, or likewise reflection.

Cross Reconstruction Loss. Following the definition of our reflection synthesis pipeline, given the predicted \hat{B}_2 and \hat{R}_1 , we should ideally be able to reconstruct the reflection input I_1 . Therefore to enhance such a constraint, we further reconstruct the cross compositions of background and reflection layers as

$$\mathcal{L}_{cross} = ||\hat{I}_{12} - I_1||_2^2 + ||\hat{I}_{21} - I_2||_2^2 \tag{4}$$

Then the network is forced to disentangle the background from reflection through the reconstruction process by specifying each output component. However, a naive solution can be easily explored by pushing all the information from the reflection image (I) into the reflection layer (R), while having the network output a black background layer of all zero values.

The naive reconstruction loss and cross reconstruction loss can be combined as

$$\mathcal{L}_{recons} = \mathcal{L}_{naive} + \mathcal{L}_{cross} \tag{5}$$

Floor Rejection Loss. To avoid the background to degenerate, we force the output background to approach the input image, as the background is usually a major subset of the input images, therefore, we define:

$$\mathcal{L}_{floor} = ||\hat{B}_1 - I_1||_2^2 + ||\hat{B}_2 - I_2||_2^2$$
 (6)

Although this objective may sound counter-intuitive since it conflicts with the above two reconstruction constraints, the network training procedure is essentially a continuous coordination and competition process of all the loss

¹Their detailed data source is introduced in the following section.

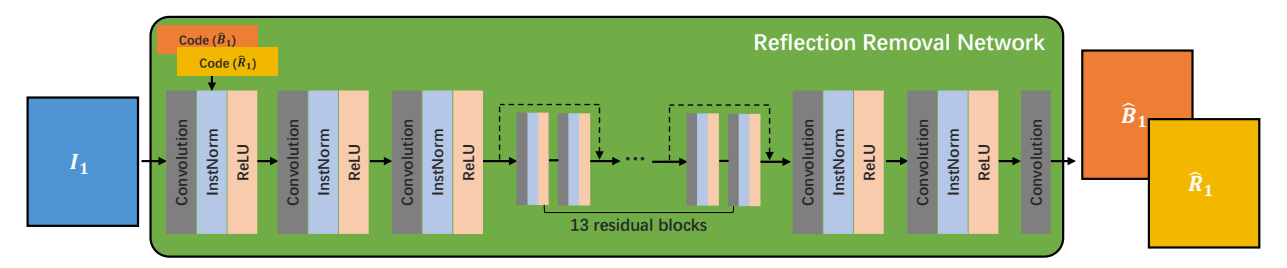


Figure 2. Our detailed reflection removal network structure. This is a one-branch fully-convolutional neural network. To enable both background and reflection prediction within such a network, we introduce the latent code defined by the learnable parameters in the first instance normalization layer to encode the output image information. To be specific, two latent codes that represent background and reflection are learned separately, and fed to the network independently to generate the corresponding output.

functions. This floor rejection loss justifies its effectiveness by prohibiting a naive solution of all-zero background, which is shown in the later ablation study section 6.2.

Ceiling Rejection Loss. The combination of the previous loss functions yields a better disentanglement, which is however still insufficient to generate a satisfactory background. As the two input reflection images are highly correlated, we take better advantage of their relationship by appending a ceiling rejection loss which prevents the background intensity from exceeding each of the two input images, reads as,

$$f(\hat{B}_1, I_1, m) = \begin{cases} ||\hat{B}_{1,m} - I_{1,m}||_1 & \hat{B}_{1,m} > I_{1,m}, \\ 0 & \text{otherwise;} \end{cases}$$
(7)

$$\mathcal{L}_{ceiling} = \sum_{m} (f(\hat{B}_1, I_1, m) + f(\hat{B}_1, I_2, m) + f(\hat{B}_2, I_1, m) + f(\hat{B}_2, I_2, m))$$
(8)

where m indicates each image pixel. The ceiling rejection loss is a summation of f among the whole image region. It sets an upper bound for each background prediction, which punishes any background pixel whose intensity value is larger than either input one.

Therefore, the overall objective function is a weighted combination of the above four loss terms, defined as

$$\mathcal{L}_{unsuper} = \lambda_1 \mathcal{L}_{recons} + \lambda_2 \mathcal{L}_{floor} + \mathcal{L}_{ceiling}$$
 (9)

where the specific value for λ_1 and λ_2 are addressed in the experiment section.

Note there is only one reflection removal network that exists in our full pipeline, and all the different inputs are fed through the same network individually. Such a design support further extension to three or more inputs without modifying the architecture. In this paper, we take only two reflection images as input for simplicity. Benefited from such a design, our framework can also be naturally switched for single image reflection removal during evaluation.

Even though no ground truth label is directly used as supervision, our framework benefits from theoretically designed objective function and learns a better reflection prior for real images as shown in the later experiment section.

4. Reflection Removal Network

In this section, we introduce the details of our reflection removal network that unifies background and reflection prediction within a one-branch pipeline. Our network structure is shown in Figure 2.

For our specialized framework, one network of multiple output branches or even two independent neural networks are usually required for both background and reflection prediction. In this paper, we develop a more elegant way to couple the background and reflection within a single network, and provide a new understanding of the learning based reflection removal approach.

Following the basic network structure in [6], our neural network is a fully convolutional neural network (FCN), which contains 32 convolution layers, where the middle 26 ones are organized into 13 residual blocks to accelerate convergence. All the convolution layers have 3×3 kernel size with output channel number as 64, and are followed by instance normalization [27] and ReLU layer except for the last one. The input and output of the network are both a three channel color image.

However, training such a one-branch fully convolutional neural network is challenging, as it does not support two concurrent outputs for a given single input image. To transform this network in a more suitable way, we introduce the latent code that explicitly learns the background or reflection information.

This latent code is implemented as the learnable parameters (scale and shift) in the first instance normalization layer, which is decoupled from the network as an independent parameterized vector. During the training process, two latent codes that represent the background and reflection are independently learned. Given a single input image, the output of the reflection removal network is determined by switching the two controllable latent codes. As the instance normal-



Figure 3. Visual comparison on the strong real-world reflection images from [6]. These images are featured by subtraction and clipping image model.

ization layer takes 64 feature maps as input, the latent code is only defined in a tiny vector of size 128. Benefited from such a design, the specific background or reflection information are all encoded into these 128 learnable parameters, while all the other network weights are shared for them.

Experimentally, we observe the best performance by selecting the first instance normalization layer, since in this manner, most subsequent layers can leverage the latent code to better differentiate the background and reflection.

5. Experiments

Due to the lack of large-scale high-quality reflection image dataset, the learning based approaches mostly synthesize reflection images for training. Currently, there are two mainstream data synthesis methods, which mainly differentiate in the logic of computing the reflection layer: (1) One of the methods is developed by [6] and followed by [39, 32]. Their reflection layer is generated via subtraction and clipping operations. It reflects some physical properties observed in natural scenes. The generated images tend to contain strong and blurry reflections. (2) The other method is the common linear additive image mixing model used by [30, 36]. Their reflection layer is only scaled by a small factor for direct composition. The resultant reflections are weaker yet sharper.

As these approaches have their specialties in image formation process and bias towards target images, we split our experiments by different training data generated from the above two synthesis methods for our algorithm².

Data source	Collected Real	SIR ²	
Error metric	%	PSNR	SSIM
Input	-	26.19	0.916
Wan et al. 2018 [30]	-	22.16	0.828
Wen et al. 2019 [33]	0.28	21.23	0.854
Yang et al. 2018 [36]	9.07	22.25	0.853
Li et al. 2014 [16]	2.97	18.87	0.782
Fan et al. 2017 [6]	8.50	20.97	0.839
Zhang et al. 2018 [39]	19.83	21.20	0.862
Wei et al. 2019 [32]	6.52	24.14	0.879
Ours (w. GT label)	18.13	24.81	0.903
Ours	34.70	22.72	0.870

Table 1. SOTA Comparison on the user study of collected strong real reflections with our subtraction model (left), and image quality evaluation of the wild scene images of SIR² dataset with our linear addition model (right).

5.1. Subtraction and Clipping Image Model

Implementation Details. Following [6], we collect around 17,000 natural images from PASCAL VOC dataset as the data source of the image synthesis approach, while 5% of them are treated as test data and the left are training data. During the network training process, we randomly sampled two images from the training/test split to synthesize the reflection images online. We directly adopt [6]'s method to generate our training data. Our framework is implemented in PyTorch. Our deep network is optimized by Adam with mini-batch size as 8. Some specifics about our training setting: initial learning rate (0.01), training epoch number (60), λ_1 (15), λ_2 (20).

Results. To evaluate our algorithm on the real images, we randomly collect around 30 reflection images that fea-

²Note [33] learns the alpha mask in the linear composition model for reflection synthesis, which we also experiment with, but doesn't work better than the image model in our problem setting.



Figure 4. Visual comparison on strong real-world reflection images collected by ourselves. These images are featured by subtraction and clipping image model.

ture strong and blurry reflections, and conduct a user study among 40 users. They are asked to pick the best visual result among 8 approaches for each example, and we evaluate the user selections for each method in Table 1³. We also experiment by replacing the proposed loss functions with the supervision losses for training on the ground truth data, denoted as "w. GT label". The corresponding qualitative results are demonstrated in Figure 3 ([6]'s test images) and 4 (self-collected images).

For both numerical and visual results, our proposed pipeline outperforms the others. Note on the visual side, our algorithm learns to remove more reflections and generate cleaner background, even compared with [39, 6, 32] that share the similar data generation approach as ours. We further test our model on the synthetic test data, and observe degraded performance compared to our fully supervised alternative. This may be because our proposed learning objective learns to have more understanding of the theoretical reflection removal process, and hence enhance the generalization to real cases.

5.2. Linear Addition Image Model

Implementation Details. Similarly to the subtraction and clipping image model, we directly take their train/test split in the PASCAL VOC dataset as our data source. We follow [36]'s approach to linearly mix two natural images with a constant scale factor to synthesize the reflection image, where the scale weight is within [0.6, 0.8] for the reflection layer. We adopt the similar training setting as in the subtraction and clipping image model. The difference lies in: training epoch number (10), λ_1 (80), λ_2 (50). The parameter change is caused by the significantly different data

generation approach.

Results. SIR² [29] is a well-known reflection removal benchmark that contains relatively weak and sharp reflections compared to the one generated by the aforementioned image formation model. We follow SIR²'s subsequent work [30], led by the same researchers, to utilize the linear addition image model to prepare for the training data, and take the wild scene images in SIR² dataset for comparison.

The numerical comparisons and its corresponding visual images are shown in Table 1 and Figure 5. Compared to the reflections in the above section, the reflections in SIR² dataset are weaker yet sharper. From the visual perspective, our approach does not only generate cleaner background, but also preserves better image structure and color.

Regarding the numerical performance, our approach overwhelms most previous approaches except for [32] and our fully supervised alternative. Note [32] observes a frustrating fact that the input reflection images achieve the best numerical error as shown in Table 1. This is potentially caused by the fact that the captured reflections are mostly weak and partially distributed in the image region, while most approaches are designed to touch the image as a whole and accidentally causes more error in the reflection-free region. For example, [39] changes the overall intensity of the test images in Figure 5. Even if some reflections are removed, many important details are also diminished and the color is wrongly shifted. Moreover, we also observe similar phenomenon on the trained synthetic data as in clipping image model.

³Due to inaccessibility to [30]'s codes or trained model, their results are not present for the subtraction and clipping image model.

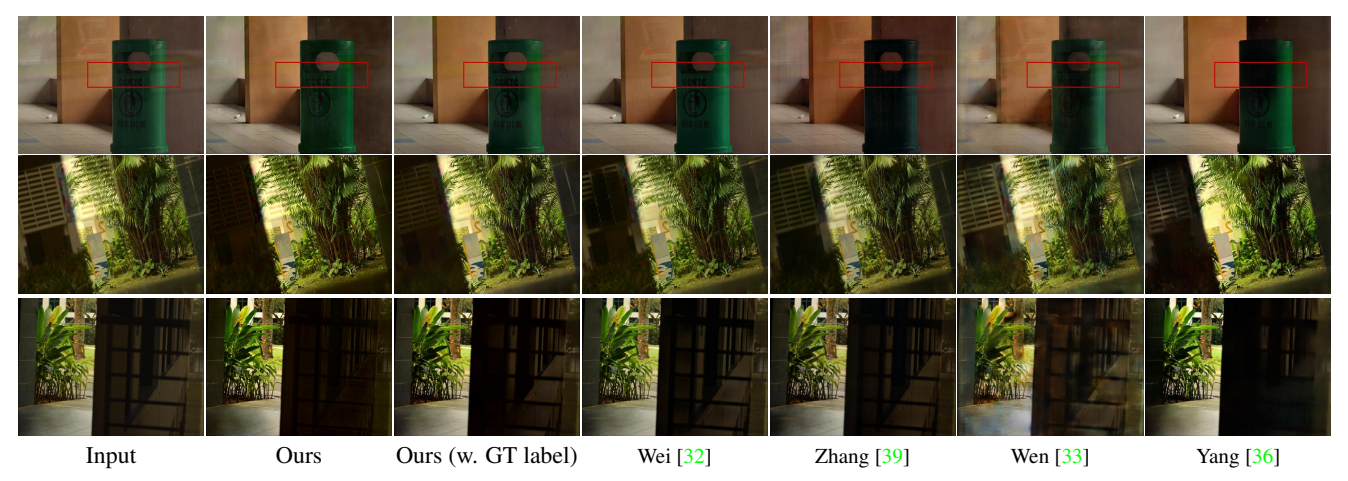


Figure 5. Visual comparison on the wild scene images of SIR² dataset. **Zoom in to see the details.**



Figure 6. Visual comparison of different alternatives of our algorithm. Zoom in to see the difference.

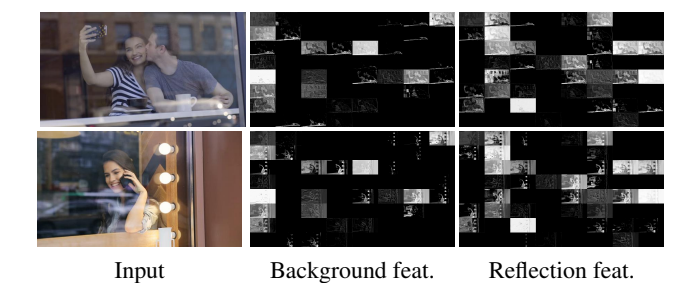


Figure 7. Visualization of background and reflection features after the first instance normalization layer where the latent code is embedded. 64 feature maps are allocated into an 8×8 block for visualization.

6. Ablation Study and Analysis

6.1. What does the latent code learn?

In our implementation, the latent code encodes the unique information for background or reflection, while the rest of network weights are shared. It means the layer separation task is conducted by the specific instance normalization layer where our learned latent code is embedded. Then we are interested in the difference between the feature maps generated by this instance normalization layer with

the background and reflection latent codes.

Analysis of Active Features. Inspired by the sparsity property of convolution features [4], we study the active feature channel for background and reflection. To achieve it, we deactivate each channel of the feature map by setting its value to all zero, and compute the difference (MSE) between the manipulated and untouched output image. We conduct such an experiment among 100 real reflection images. As long as the average MSE is larger than 0, this feature channel is considered "active" for output generation.

As a result, among all 64 feature maps, interestingly we find that only 35 channels are active for background, and 40 channels for reflection, while eliminating all the other channels does not influence the output generation. Moreover, the background and reflection share only 20 common active channels. However, active channel is not always effective. When filtering out the "ineffective" ones (average MSE < 1), there are only 11 overlapped channels. It means that the learned latent code differentiates background and reflection by allocating different active feature maps.

To further justify the above observation, we visualize the normalized feature maps of two randomly picked real images in Figure 7. As shown in this figure, many feature

	\mathcal{L}_{recons}	$\mathcal{L}_{recons} + \mathcal{L}_{floor}$	Split feature	6-channel output	Two networks	More inputs	Full pipeline
PSNR	6.20	16.44	16.98	17.06	17.76	17.35	17.92
SSIM	0.012	0.804	0.824	0.813	0.823	0.841	0.842

Table 2. Ablation study on the synthetic test data generated by the subtraction and clipping image model.

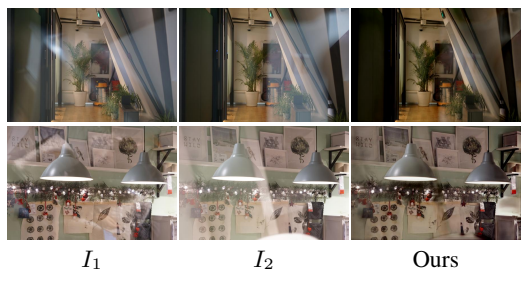


Figure 8. Visual results of our algorithm learned on the real labelfree reflection data.

maps are totally blank while only part of them contain color intensities. And the active background and reflection feature maps are mostly different from each other. Similar phenomenon is consistently observed in many more examples. **Feature Splitting.** Inspired by this observation, we learn to unify background and reflection predictions into one network by explicitly splitting features, instead of learning latent code. Specifically, we assign half of the 64 feature maps after the first convolution layer for background by setting the other half features to all zero, and vice versa for reflection. Therefore, during training, latent code is not learned, but replaced by allocating features explicitly.

We train such a network using the subtraction and clipping image model, and demonstrate its visual results in Figure 6. Compared to our result, this feature splitting network removes much less reflections. We believe this may be because the half-half splitting of features does not reflect the ideal feature distribution, while our approach is able to adaptively learn the best feature amount for both background and reflection. A corresponding numerical comparison is shown in Table 2.

6.2. How important is each loss?

To analyze the effectiveness of each loss function, we train our network with (1) the reconstruction loss only (\mathcal{L}_{recons}) , and (2) both the reconstruction and floor rejection loss $(\mathcal{L}_{recons} + \mathcal{L}_{floor})$.

As shown in Figure 6, their visual result is far from comparable to ours. While training with the reconstruction loss only, the background is learned to be completely black, which is consistent with our analysis in section 3. Note the reconstruction loss helps differentiate the background and reflection output, even if its predicted background does not show any meaningful information. While jointly training with the floor rejection loss, the resultant image is not black any more and instead removes the reflections partially. Fi-

nally, when all the loss functions are combined together for supervision, our result is the best.

6.3. Replacement for latent code?

Instead of learning latent code within one single network, one alternative solution is to directly learn two networks for background and reflection separately. As shown in Figure 6, this two-network solution shows very similar visual results, in comparison to our proposed one-network solution. It demonstrates our efficiency by learning a single network to achieve similar performance with two networks.

Another naive replacement is to directly learn a single network with a 6-channel output, where the half are for background and the other half are for reflection. The predicted background from this trained network still contains many obvious reflections, which do not exist in our result. It justifies the effectiveness of our specific network design.

6.4. More inputs to the network?

During the implementation of our specialized framework, we take only two inputs for simplicity. But theoretically, our framework is able to take unlimited inputs. To explore its performance, we experiment by feeding three reflection images to our neural network in the training phase, whose results are shown in Figure 6.

It also demonstrates similar visual results to ours. It means that our two-input pipeline learns sufficiently good reflection removal effects, while feeding more inputs does not have significant impact in the output. We also fed more input images to the network, however it does not make substantial difference in the result.

6.5. What if training on real images?

The experiments we conduct until now all leverage the ground truth to synthesize training reflections due to the difficulty of collecting large-scale real-reflection pairs. To explore the limit of our algorithm on the real label-free reflection training data, we capture some image sequences where the background holds mostly steady and the reflection differs. Since the real image number is limited, our network is trained on each image pair iteratively, and generates the corresponding background in Figure 8. In this case, even without ground truth to synthesize perfect training pairs, our algorithm is still able to remove reflections very well. More results are given in the supplemental materials.

7. Conclusion

In this paper, we propose a learning-based approach for reflection removal problem. Our deep network learns to optimize a combination of multiple objective functions, which take advantage of relationship between multiple input images during the training phase, and transfers the learned deep reflection prior in the evaluation stage with only a single input image.

References

- A. Agrawal, R. Raskar, S. K. Nayar, and Y. Li. Removing photography artifacts using gradient projection and flash-exposure sampling. *ACM Transactions on Graphics (TOG)*, 24(3):828–835, 2005.
- [2] N. Arvanitopoulos, R. Achanta, and S. Susstrunk. Single image reflection suppression. In *Proceedings of the IEEE Conference on Computer Vision and Pattern Recognition*, pages 4498–4506, 2017.
- [3] Y. Chang and C. Jung. Single image reflection removal using convolutional neural networks. *IEEE Transactions on Image Processing*, 28(4):1954–1966, 2019. 2
- [4] D. Chen, L. Yuan, J. Liao, N. Yu, and G. Hua. Stylebank: An explicit representation for neural image style transfer. In *Pro*ceedings of the IEEE Conference on Computer Vision and Pattern Recognition, pages 1897–1906, 2017. 7
- [5] Y. Chen, W. Li, X. Chen, and L. V. Gool. Learning semantic segmentation from synthetic data: A geometrically guided input-output adaptation approach. In *Proceedings of the IEEE Conference on Computer Vision and Pattern Recognition*, pages 1841–1850, 2019.
- [6] Q. Fan, J. Yang, G. Hua, B. Chen, and D. Wipf. A generic deep architecture for single image reflection removal and image smoothing. In *Proceedings of the IEEE International Conference on Computer Vision*, pages 3238–3247, 2017. 1, 2, 4, 5, 6
- [7] H. Farid and E. H. Adelson. Separating reflections and lighting using independent components analysis. In *IEEE Conference on Computer Vision and Pattern Recognition (CVPR)*, volume 1, pages 262–267, 1999. 2
- [8] K. Gai, Z. Shi, and C. Zhang. Blind separation of superimposed moving images using image statistics. *IEEE Trans*actions on Pattern Analysis and Machine Intelligence (T-PAMI), 34(1):19–32, 2012. 2
- [9] X. Guo, X. Cao, and Y. Ma. Robust separation of reflection from multiple images. In *IEEE Conference on Computer Vision and Pattern Recognition (CVPR)*, pages 2187–2194, 2014.
- [10] N. Kong, Y.-W. Tai, and J. S. Shin. A physically-based approach to reflection separation: from physical modeling to constrained optimization. *IEEE Transactions on Pattern Analysis and Machine Intelligence (T-PAMI)*, 36(2):209– 221, 2014. 2
- [11] A. Levin and Y. Weiss. User assisted separation of reflections from a single image using a sparsity prior. *IEEE Transactions on Pattern Analysis and Machine Intelligence (T-PAMI)*, 29(9), 2007. 2

- [12] A. Levin, A. Zomet, and Y. Weiss. Learning to perceive transparency from the statistics of natural scenes. In Advances in Neural Information Processing Systems, pages 1271–1278, 2003.
- [13] A. Levin, A. Zomet, and Y. Weiss. Separating reflections from a single image using local features. In *Proceedings* of the 2004 IEEE Computer Society Conference on Computer Vision and Pattern Recognition, 2004. CVPR 2004., volume 1, pages I-I. IEEE, 2004. 2
- [14] S. Li, I. B. Araujo, W. Ren, Z. Wang, E. K. Tokuda, R. H. Junior, R. Cesar-Junior, J. Zhang, X. Guo, and X. Cao. Single image deraining: A comprehensive benchmark analysis. In *Proceedings of the IEEE Conference on Computer Vision and Pattern Recognition*, pages 3838–3847, 2019. 1
- [15] Y. Li and M. S. Brown. Exploiting reflection change for automatic reflection removal. In *IEEE International Conference on Computer Vision (ICCV)*, pages 2432–2439, 2013.
- [16] Y. Li and M. S. Brown. Single image layer separation using relative smoothness. In *IEEE Conference on Computer Vision and Pattern Recognition (CVPR)*, pages 2752–2759, 2014. 1, 2, 5
- [17] A. Nandoriya, M. Elgharib, C. Kim, M. Hefeeda, and W. Matusik. Video reflection removal through spatio-temporal optimization. In *Proceedings of the IEEE International Conference on Computer Vision*, pages 2411–2419, 2017.
- [18] B. Sarel and M. Irani. Separating transparent layers through layer information exchange. In *European Conference on Computer Vision (ECCV)*, pages 328–341, 2004. 2
- [19] Y. Y. Schechner, N. Kiryati, and R. Basri. Separation of transparent layers using focus. *International Journal of Computer Vision (IJCV)*, 39(1):25–39, 2000.
- [20] Y. Y. Schechner, J. Shamir, and N. Kiryati. Polarization and statistical analysis of scenes containing a semireflector. *JOSA A*, 17(2):276–284, 2000. 2
- [21] Y. Shih, D. Krishnan, F. Durand, and W. T. Freeman. Reflection removal using ghosting cues. In *IEEE Conference on Computer Vision and Pattern Recognition (CVPR)*, pages 3193–3201, 2015.
- [22] S. N. Sinha, J. Kopf, M. Goesele, D. Scharstein, and R. Szeliski. Image-based rendering for scenes with reflections. ACM Transactions on Graphics (TOG), 31(4):100–1, 2012. 2
- [23] O. Springer and Y. Weiss. Reflection separation using guided annotation. In 2017 IEEE International Conference on Image Processing (ICIP), pages 1192–1196. IEEE, 2017. 2
- [24] R. Sun, X. Zhu, C. Wu, C. Huang, J. Shi, and L. Ma. Not all areas are equal: Transfer learning for semantic segmentation via hierarchical region selection. In *Proceedings of the IEEE Conference on Computer Vision and Pattern Recogni*tion, pages 4360–4369, 2019. 1
- [25] R. Szeliski, S. Avidan, and P. Anandan. Layer extraction from multiple images containing reflections and transparency. In *IEEE Conference on Computer Vision and Pattern Recognition (CVPR)*, volume 1, pages 246–253, 2000.
- [26] J. Tremblay, A. Prakash, D. Acuna, M. Brophy, V. Jampani, C. Anil, T. To, E. Cameracci, S. Boochoon, and S. Birchfield.

- Training deep networks with synthetic data: Bridging the reality gap by domain randomization. In *Proceedings of the IEEE Conference on Computer Vision and Pattern Recognition Workshops*, pages 969–977, 2018. 1
- [27] D. Ulyanov, A. Vedaldi, and V. Lempitsky. Instance normalization: The missing ingredient for fast stylization. arXiv preprint arXiv:1607.08022, 2016. 4
- [28] R. Wan, B. Shi, L.-Y. Duan, A.-H. Tan, W. Gao, and A. C. Kot. Region-aware reflection removal with unified content and gradient priors. *IEEE Transactions on Image Processing*, 27(6):2927–2941, 2018. 2
- [29] R. Wan, B. Shi, L.-Y. Duan, A.-H. Tan, and A. C. Kot. Benchmarking single-image reflection removal algorithms. In *Proceedings of the IEEE International Conference on Computer Vision*, pages 3922–3930, 2017. 6
- [30] R. Wan, B. Shi, L.-Y. Duan, A.-H. Tan, and A. C. Kot. Crrn: multi-scale guided concurrent reflection removal network. In Proceedings of the IEEE Conference on Computer Vision and Pattern Recognition, pages 4777–4785, 2018. 1, 2, 5,
- [31] R. Wan, B. Shi, T. A. Hwee, and A. C. Kot. Depth of field guided reflection removal. In *Image Processing (ICIP)*, 2016 IEEE International Conference on, pages 21–25. IEEE, 2016. 2
- [32] K. Wei, J. Yang, Y. Fu, D. Wipf, and H. Huang. Single image reflection removal exploiting misaligned training data and network enhancements. In *Proceedings of the IEEE Conference on Computer Vision and Pattern Recognition*, pages 8178–8187, 2019. 1, 5, 6, 7
- [33] Q. Wen, Y. Tan, J. Qin, W. Liu, G. Han, and S. He. Single image reflection removal beyond linearity. In *Proceedings of the IEEE Conference on Computer Vision and Pattern Recognition*, pages 3771–3779, 2019. 1, 5, 7
- [34] P. Wieschollek, O. Gallo, J. Gu, and J. Kautz. Separating reflection and transmission images in the wild. In *Proceedings of the European Conference on Computer Vision (ECCV)*, pages 89–104, 2018. 2
- [35] T. Xue, M. Rubinstein, C. Liu, and W. T. Freeman. A computational approach for obstruction-free photography. ACM *Transactions on Graphics (TOG)*, 34(4):79, 2015. 1, 2
- [36] J. Yang, D. Gong, L. Liu, and Q. Shi. Seeing deeply and bidirectionally: A deep learning approach for single image reflection removal. In *Proceedings of the European Conference on Computer Vision (ECCV)*, pages 654–669, 2018. 1, 2, 5, 6, 7
- [37] J. Yang, H. Li, Y. Dai, and R. T. Tan. Robust optical flow estimation of double-layer images under transparency or reflection. In *IEEE Conference on Computer Vision and Pat*tern Recognition (CVPR), pages 1410–1419, 2016. 2
- [38] Y. Yang, W. Ma, Y. Zheng, J.-F. Cai, and W. Xu. Fast single image reflection suppression via convex optimization. *arXiv* preprint arXiv:1903.03889, 2019. 1, 2
- [39] X. Zhang, R. Ng, and Q. Chen. Single image reflection separation with perceptual losses. In *Proceedings of the IEEE Conference on Computer Vision and Pattern Recognition*, pages 4786–4794, 2018. 1, 2, 5, 6, 7